СТРОИТЕЛЬНАЯ МЕХАНИКА ИНЖЕНЕРНЫХ КОНСТРУКЦИЙ И СООРУЖЕНИЙ
STRUCTURAL MECHANICS OF ENGINEERING CONSTRUCTIONS AND BUILDINGS

2025. 21(5). 474–494

ISSN 1815-5235 (Print), 2587-8700 (Online)
HTTP://JOURNALS.RUDN.RU/STRUCTURAL-MECHANICS

DOI: 10.22363/1815-5235-2025-21-5-474-494
EDN: DGNKGJ

Research article / Научная статья

# Thermomechanical Performance of Steel and Recycled Aluminium Plates in Tropical Savanna Climatic Conditions

**Paschal Ch. Chiadighikaobi**✉, **Obumneme C. Onuoha**, **Akintomiwa E. Fagbuyi**

Afe Babalola university, *Ado-Ekiti, Ekiti state, Nigeria*
✉ chiadighikaobi.paschalc@abuad.edu.ng

Received: May 13, 2025
Revised: August 7, 2025
Accepted: September 12, 2025

**Abstract.** This research covers and compares the thermomechanical behavior of steel and recycled aluminium plates under concentrated loading and buckling conditions in several thermal conditions simulating the tropical savanna (Aw) climate. The study aims to explore their structural behavior as a function of temperature and evaluate their applicability in heat-sensitive applications. Finite element analysis (FEA) was used to model the buckling and deformation behavior of the two materials at temperatures from 0°C to 44°C and uniaxial loading of up to 100 MPa. The analytical and numerical solutions were compared; their results would differ no more than 5%, thus validating the FEA model. The steel plates generally buckled less (greater critical buckling load) in hotter thermal conditions than the aluminium. The buckling load of steel reduced by approximately 40% in Mode 1 when it went from 33°C to 44°C, while the buckling load of aluminium reduced by just 4.71%. The same trend was observed in Mode 2. These findings validate that recycled aluminium possesses superior thermomechanical stability to tropical thermal fluctuation and can be a good alternative as a material for structures in applications of high thermal fluctuation, which will be beneficial towards maximum utilization of resources in building engineering.

**Keywords:** loss of stability, critical load, deformation, recycled aluminium plates, steel plate

**Conflicts of interest.** The authors declare no conflict of interest, financial or otherwise.

**Authors' contribution:** *Chiadighikaobi P.Ch.* — concept, methodology, analysis, software, supervision, project administration, validation; *Onuoha O.C.*— conceptualization, methodology, software, text writing; *Fagbuyi A.E.* — review and editing, data interpretation. All authors have read and approved the final version of the manuscript.

**For citation:** Chiadighikaobi P.Ch., Onuoha O.C., Fagbuyi A.E. Thermomechanical performance of steel and recycled aluminium plates in tropical savanna climatic conditions. *Structural Mechanics of Engineering Constructions and Buildings*. 2025;21(5): 474–494. http://doi.org/10.22363/1815-5235-2025-21-5-474-494 EDN: DGNKGJ

***Paschal Ch. Chiadighikaobi,*** Ph.D., M.Sc., Senior lecturer in the Department of Civil engineering, Afe Babalola University, Ado-Ekiti, Ekiti State, Nigeria; ORCID: 0000-0002-4699-8166; e-mail: chiadighikaobi.paschalc@abuad.edu.ng

***Obumneme C. Onuoha,*** Graduate of the Department of Civil Engineering, Afe Babalola University, Ado-Ekiti, Ekiti State, Nigeria; ORCID: 0009-0003-7191-1581; e-mail:Obumonu45@gmail.com

***Akintomiwa E. Fagbuyi***, Graduate of the Department of Civil Engineering, Afe Babalola University, Ado-Ekiti, Ekiti State, Nigeria ; ORCID: 0009-0002-0694-1728; e-mail:akinfagbuyi@gmail.com

# Термомеханические характеристики пластин из стали и переработанного алюминия в климатических условиях тропической саванны

**П.Ч. Чиадигхикаоби ✉, О.С. Онуоха, А.Э. Фагбуйи**

Университет Афе Бабалола, *Адо-Экити, штат Экити, Нигерия*
✉ chiadighikaobi.paschalc@abuad.edu.ng

Поступила в редакцию: 13 мая 2025 г.
Доработана: 7 августа 2025 г.
Принята к публикации: 12 сентября 2025 г

**Аннотация.** Рассмотрены и сравнены термомеханические характеристики пластин из стали и переработанного алюминия в условиях действия сосредоточенной нагрузки и потери устойчивости при нескольких температурных режимах, имитирующих климат тропической саванны. Цель исследования — изучение их прочностных характеристик в зависимости от температуры и оценка их применимости в термочувствительных областях. Для моделирования поведения двух материалов при потере устойчивости и деформировании при температурах от 0 °C до 44 °C и одноосной нагрузке до 100 МПа использован метод конечного элемента. Проведено сравнение аналитических и численных решений; их результаты отличались не более чем на 5 %, что подтвердило точность конечно-элементной модели. Стальные пластины, как правило, были более устойчивы (вызывающая потерю устойчивости критическая нагрузка выше) при повышенной температуре, чем алюминиевые. При повышении температуры с 33 до 44 °C критическая нагрузка стали в режиме 1 снизилась примерно на 40 %, в то время как критическая нагрузка алюминия снизилась лишь на 4,71 %. Аналогичная тенденция наблюдалась и в режиме 2. Эти результаты подтверждают, что переработанный алюминий обладает превосходной термомеханической устойчивостью к тропическим температурным колебаниям и может быть хорошей альтернативой в качестве материала для конструкций в условиях высоких температурных колебаний, что будет способствовать максимальному использованию ресурсов в строительстве.

**Ключевые слова:** потеря устойчивости, критическая нагрузка, деформация, переработанные алюминиевые пластины, стальные пластины

**Заявление о конфликте интересов.** Авторы заявляют об отсутствии конфликта интересов, финансового или иного характера.

**Вклад авторов:** *Чиадигхикаоби П.Ч.* — концепция, методология, расчет, программная реализация, руководство, управление проектом, валидация; *Онуоха О.С.* — концептуализация, методология, программная реализация, написание текста; *Фагбуйи А.Э.* — рецензирование и редактирование, интерпретация данных. Все авторы прочитали и одобрили окончательный вариант рукописи.

**Для цитирования:** *Chiadighikaobi Ph.Ch., Onuoha O.C., Fagbuyi A.E.* Thermomechanical performance of steel and recycled aluminium plates in tropical savanna climatic conditions // Строительная механика инженерных конструкций и сооружений. 2025. Т. 21. № 5. С. 474–494. http://doi.org/10.22363/1815-5235-2025-21-5-474-494 EDN: DGNKGJ

## 1. Introduction

The thermomechanical properties of materials are a dominant factor in defining their suitability in structural systems under varying climate conditions of tropical savanna regions. Steel is the most favoured material for load-carrying structures due to its increased strength, ductility, and proven reliability. But the highly corrosive tendencies of steel have resulted in the continuous search for alternative materials. From the integration of fibre-reinforced polymers to the use of recycled plastic bricks, several materials have been explored, with their mechanical properties analysed to obtain the potential advantages and limitations. Among these alternatives, aluminium has gained considerable attention. Aluminium is resistant to corrosion and has been used as an adequate replacement for steel in some specific conditions globally.

Beyond its mechanical advantages, the consideration of aluminium also extends to issues of material availability and life cycle utilization. Waste management has a significant environmental impact [1]. The

***Чиадигхикаоби Паскал Чимеремезе,*** доктор философии, магистр наук, старший преподаватель кафедры гражданского строительства, Университет Афе Бабалола, Адо-Экити, штат Экити, Нигерия; ORCID: 0000-0002-4699-8166; e-mail: chiadighikaobi.paschalc@abuad.edu.ng

***Онуоха Обумнем С.***, аспирант факультета гражданского строительства, Университет Афе Бабалола, Адо-Экити, штат Экити, Нигерия; ORCID: 0009-0003-7191-1581; e-mail: Obumonu45@gmail.com

***Фагбуйи Акинтомива***, аспирант факультета гражданского строительства, Университет Афе Бабалола, Адо-Экити, штат Экити, Нигерия; ORCID: 0009-0002-0694-1728; e-mail: akinfagbuyi@gmail.com

disposal of aluminium cans, commonly used for soft drinks, has become one of the prevailing issues. These cans are found littering the environment, adding to pollution and waste management challenges, as they cannot be easily decomposed. This condition presents a dual challenge: addressing environmental pollution and finding sustainable uses for these waste materials. Repurposing these aluminium cans into components for aluminium plates in construction is a sustainable solution. This approach aids in reducing environmental pollution and contributes to the development of eco-friendly construction materials.

The widespread use of aluminium cans can be traced back to advancements in food science. Today, aluminium cans are considered a conventional means of packaging food and beverages for commercial consumption. Previously, glass dominated the drink packaging market until the late 1950s.[3] The first all-aluminium beverage cans were introduced in 1958 by the Hawaii Brewing Company for their "Primo Beer".[4] Aluminium has increasingly been used as a method of canning due to its low weight, low cost, and recyclability. "The world's beer and soda consumption uses about 180 billion aluminium cans every year. This is 6,700 cans per second, enough to go around the planet every 17 hours".[5] Aluminium cans are made from a combination of elements to form an aluminium alloy. The chemical makeup of this alloy varies. Table 1 summarises the chemical makeup of aluminium alloys.

*Table 1*

**Chemical makeup of aluminium alloy**

| Element | Symbol | Percentile make-up, % |
|---|---|---|
| Aluminium | Al | 93.75 – 96.46 |
| Magnesium | Mg | 2.53 – 4.82 |
| Manganese | Mn | 0.27 – 0.33 |
| Iron | Fe | 0.26 – 0.32 |

S o u r c e: compiled by V.Y. Risonarta et al. [2].

The first step in recycling aluminium cans involves the collection and sorting of aluminium cans based on alloy type, grade, and other factors. This sorting process can be done manually or using technologies like eddy current separators, air classifiers, and density separators. After sorting, the aluminium cans are shredded and cleaned to remove any impurities or coatings. The cleaned aluminium scrap is then melted in a furnace at high temperatures, typically around 660 °C. The molten metal is poured into ingot casts to set. Alloy formulas are chosen based on the planned uses for the reprocessed aluminium. Lastly, the resulting ingots can be transported to aluminium processing or manufacturing plants to be made into new products, including structural aluminium alloy [3–6]. Although aluminium is a highly recyclable material, there are only a few recycling industries in Africa.

In Nigeria, for instance, an estimated 87% of aluminium cans are left unrecycled. Reports show that only 13 percent of recyclable goods are salvaged and recycled in Nigeria, with almost no formal waste diversion process in place.[6] The process of recycling aluminium cans into structural aluminium alloys must be given great attention; poorly recycled alloys will produce underperforming materials.

The application of aluminium in civil engineering is dependent on the physical and mechanical properties (see Table 2) of the alloy. These properties include density, elastic modulus, ultimate strength, Poisson ratio, etc.

[3] The History of Metal Packaging | A brief overview of metal packaging. 2019. Available from: https://www.shilohplastics.com.au/history-of-metal-packaging/ (accessed: 14.04.2025)

[4] Svendsen A. 60 years of the Aluminium Can — Light Metal Age Magazine. 2018. Available from: https://www.lightmetalage.com/news/industry-news/applications-design/60-years-of-the-Aluminium-can/ (accessed: 14.04.2025)

[5] The world counts. (n.d.). Available from: https://www.theworldcounts.com/challenges/consumption/foods-and-beverages/aluminium-cans-facts. (accessed: 14.04.2025)

[6] Aluminium recycling in Africa is an opportunity for big business, Op-Ed by Raymond Onovwigun | Romco Metals. 2022. Available from: https://romcometals.com/aluminium-recycling-in-africa-is-an-opportunity-for-big-business/(accessed: 03.04.2025).

*Table 2*

**Aluminium properties**

| Properties | Symbol | 5005-H12 Aluminium | 6005-T1 Aluminium |
|---|---|---|---|
| Density, kg/m$^3$ | $Q$ | 2,660 | 2,770 |
| Elastic Modulus, MPa | $E$ | 70,300 | 71,000 |
| Poisson's Ratio | $v$ | 0.30 | 0.33 |
| Ultimate Strength, MPa | $Ru$ | 275 | 310 |

S o u r c e: compiled by Z. Zuo et al. [7].

The integration of aluminium alloys in civil engineering has been in existence for more than 80 years. First used in the design and construction of static transport structures like bridges, from the reconstruction of Pittsburgh's bridge roadway project in 1933 to the construction of New York's railway bridge in 1946. This work fostered the construction of other global aluminium-aided structures as well as the development of various international standard codes guiding their design [8]. The United States primarily uses the Aluminium Design Manual (ADM) as guidance in the design of aluminium structures [9]. While BS 8118-1:1991 is the "Code of Practice for the Structural Use of Aluminium" and was one of the first codes to be written in limit state format for aluminium design[7], and BS EN 1999-1-1:2007 provides the guidelines and specifications for the design of aluminium structures within the European Union[8]. Aluminium has been utilised in some major projects globally to solve various structural and environmental issues; aluminium alloy was used in the reconstruction of the Real Ferdinando bridge decking in Italy to reduce the self-weight of the bridge. Likewise, pure aluminium can be used in passive seismic protection systems due to its low yield strength and high degree of ductility. Furthermore, the integration of aluminium alloys is necessary for structures exposed to extreme temperature variations. Aluminium lacks negative implications related to brittleness at low temperatures compared to steel [8]. Aluminium is also utilized in the design of plates and shell-like structural elements. For example, the design and construction of bridges, roofs, walls, box culverts, pipe arches, silos, tanks, cooling towers, reactor vessels, culverts, storm sewers, service tunnels, recovery tunnels, stream enclosures, and underpasses[9] [10].

Despite the various advancements in international codes and multiple uses of aluminium globally, there remains a limited understanding of the effect of temperature on the deformation and buckling behaviour of aluminium plates under load. Bridging this knowledge gap is key to exploiting the full potential of the material in varying climatic conditions. As the world grapples with the challenges of urbanisation and a growing population, the demand for durable and environmentally responsible construction materials has never been more pressing. This paper reviewed several relevant articles and textbooks acquired with the aid of multiple research databases, i.e. Google Scholar, Scopus, etc. to validate the accuracy of the theories and finite element analysis (FEA) carried out in this study. FEA tool (ANSYS) was used to run a comparative analysis on aluminium and steel plates under simulated real-world scenarios.

### *1.1. Aluminium Plates*

The recycled aluminium from aluminium cans can be forged into a variety of structural elements, like plates. A plate is a structural element that is characterised by a three-dimensional solid whose thickness is small in comparison to its other dimensions [11]. Plates serve various functions, such as providing stable surfaces for floors, roofs, and walls, as well as distributing loads efficiently throughout a structure[10] . Plates

[7] BS 8118-1. (1991). Structural use of aluminium — Code of practice for design.

[8] EN 1999-1-1 (2007) (English): Eurocode 9: Design of aluminium structures — Part 1-1: General structural rules.

[9] Aluminium structural Plate by Contech Engineered Solutions. (n.d.). — Contech Engineered Solutions. https://www.contech.com/bridges-structures/plate/Aluminium-structural-plate/

[10] Plates. (n.d.). The structural engineer. Available from: https://www.thestructuralengineer.info/education/structural-systems/plates (accessed: 03.04.2025).

can also be defined as planar, two-dimensional components that primarily transfer forces in the direction of their plane. Plates are greatly utilised in structures in the form of floors and walls. The wall plate elements in buildings are used to transfer all vertical loads as axial forces into the foundation; they ensure the horizontal stiffening of the entire structure [12; 13].

The deformation and structural behavior of a plate under loading are dependent on the plate's material properties. Furthermore, the effects of loads on plates generate stresses predominantly normal to the element's thickness, and their mechanics are the main subject of plate theory [11]. Plate theory aims to calculate deformation and stress in a plate subjected to loads. There are two widely accepted plate theories used: the Kirchhoff-Love theory of plates (classical plate theory) and the Reissner-Mindlin theory of plates (first-order shear plate theory) [14; 15].

The Reissner-Mindlin theory is applied for thick plates, where the shear deformation and rotary inertia effects are included [14], while the Kirchhoff-Love theory is an extension of the Euler-Bernoulli beam theory to thin plates. There are three assumptions made in the Kirchhoff-Love theory. Firstly, the mid-plane is a "neutral plane," like in beam theory. Secondly, line elements remain normal to the mid-plane. Finally, vertical strain is ignored, meaning that the thickness of the plate does not change during deformation (see Figure 1) [14; 15].

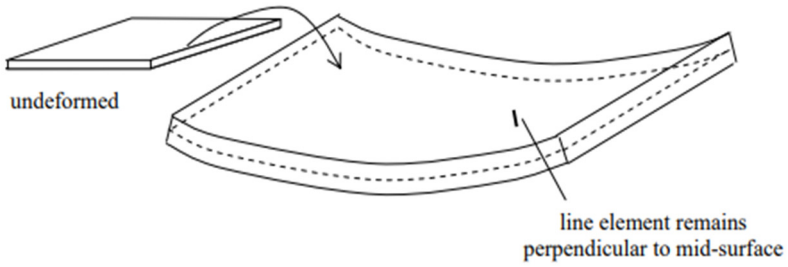


**Figure 1.** Deformed line elements remain perpendicular to the mid-plane
S o u r c e: compiled by Kelly. (n.d.). Plate theory[11].

Under loading, stresses are generated on and within the plate, causing bending. The bending of the plate helps to resist the applied load on the plate. In addition, the bending of the plate is greatly influenced by the Poisson ratio of the material. The smaller the Poisson ratio of the plate material, the more the loading would produce a more singly curved, deformed surface, as seen in Figure 2, *a*. However, if the plate material has a non-zero Poisson's ratio, the deflected shape will be as shown in Figure 2, *b*. Therefore, most aluminium alloy plates would have greater deformation than steel plates [17].

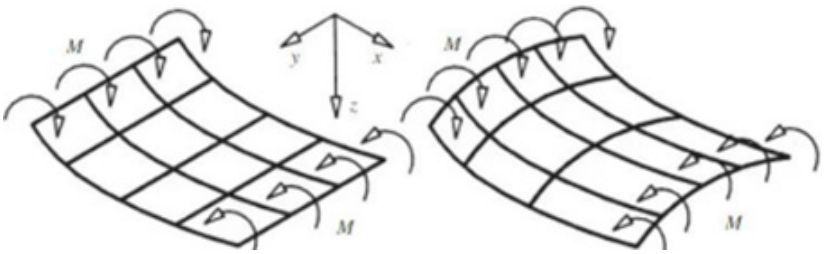


*a* *b*

**Figure 2.** Deformed surface of a plate with:
*a* — low Poisson's ratio; *b* — high Poisson's ratio
S o u r c e: compiled by D. Johnson [17].

[11] Kelly. (n.d.). Plate theory. In Solid Mechanics Part II (pp. 120–126). Available from: https://pkel015.connect.amazon.auckland.ac.nz/SolidMechanicsBooks/Part_II/06_PlateTheory/06_PlateTheory_Complete.pdf

Other factors that influence the magnitude of deformation of a plate under loading are shapes, support conditions, and the type of loading the plate is subjected to (see Table 3) and Equations (1)–(8).

*Table 3*

**Maximum deformation of plate formulae**

| Shape of plate | Support conditions & Type of load | Max deformation (at centre) |
|---|---|---|
| Circular | Edges are simply supported & uniformly loaded 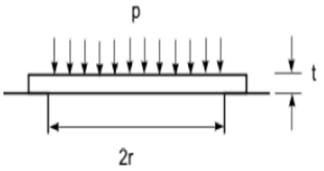  | $y_m = \frac{(5+v)\,pr^4}{64(1+v)D}$ (1) |
| Circular | Edges clamped & uniform load 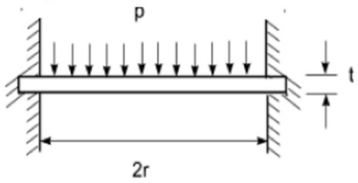  | $y_m = \frac{pr^4}{64D}$ (2) |
| Circular | Edges simply supported & concentrated load 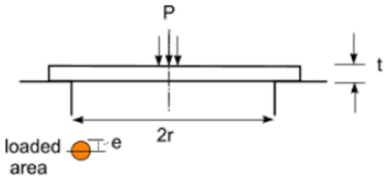  | $y_m = \frac{(3+v)\,Pr^2}{16\pi(1+v)D}$ (3) |
| Circular | Edges clamped & concentrated load 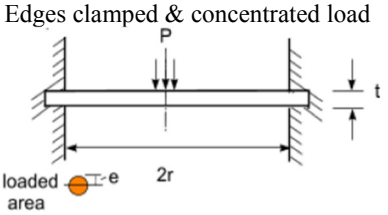  | $y_m = \frac{Pr^2}{16\pi D}$ (4) |
| Rectangular | Edges simply supported & uniform load 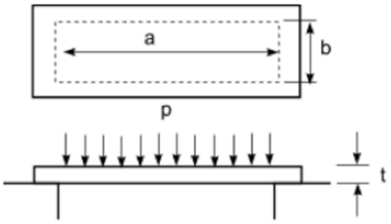  | $y_m = \frac{0.142\,pb^4}{Et^3\left(2.21(b/a)^3+1\right)}$ (5) |
| Rectangular | Edges clamped & uniform load 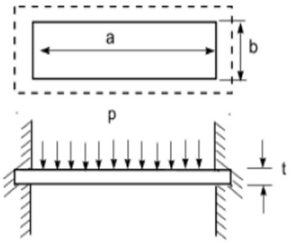  | $y_m = \frac{0.0284\,pb^4}{Et^3\left(1.056(b/a)^5+1\right)}$ (6) |

*Ending of the Table 3*

<table>
<tr><th>Shape of plate</th><th>Support conditions & Type of load</th><th>Max deformation (at centre)</th></tr>
<tr><td>Rectangular</td><td>Edges simply supported & concentrated load<br> 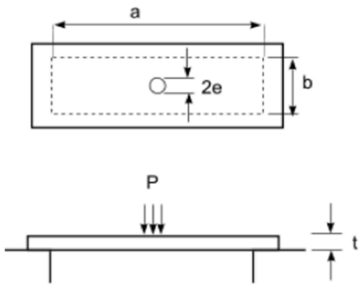 </td><td>$y_m = k_1 \frac{Pb^2}{Et^3}$ (7)<br><table><tr><th>$(a/b)$</th><th>$k_1$</th><th>$(a/b)$</th><th>$k_1$</th></tr><tr><td>1.0</td><td>0.127</td><td>1.6</td><td>0.17</td></tr><tr><td>1.1</td><td>0.138</td><td>1.8</td><td>0.177</td></tr><tr><td>1.2</td><td>0.148</td><td>2.0</td><td>0.180</td></tr><tr><td>1.4</td><td>0.162</td><td><3.0</td><td>0.185</td></tr></table></td></tr>
<tr><td>Rectangular</td><td>Edges clamped & concentrated load<br> 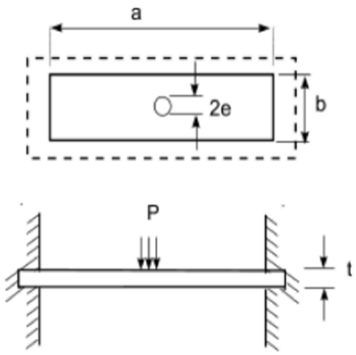 </td><td>$y_m = k_1 \frac{Pb^2}{Et^3}$ (8)<br><table><tr><th>$(a/b)$</th><th>$k_1$</th><th>$(a/b)$</th><th>$k_1$</th></tr><tr><td>1.0</td><td>0.061</td><td>1.8</td><td>0.0786</td></tr><tr><td>1.2</td><td>0.071</td><td>2.0</td><td>0.0788</td></tr><tr><td>1.4</td><td>0.076</td><td><3.0</td><td>0.0791</td></tr><tr><td>1.6</td><td>0.078</td><td></td><td></td></tr></table></td></tr>
</table>

S o u r c e: compiled by Loaded Flat Plates. (n.d.). Roymech Loaded Flat Plates. (n.d.). Roymech. Available from: https://www.roymech.co.uk/Useful_Tables/Mechanics/Plates.html (accessed: 03.04.2025).

where $r$ is the radius of the circular plate (m); $a$ is the major length of the rectangular plate (m); $b$ is the minor length of the rectangular plate (m); $t$ is plate thickness (m); $p$ is uniform surface pressure on the plate (compressive) (N/m$^2$); $P$ is single concentrated force (compressive) (N); $y_m$ is the maximum deformation (m); $E$ = Young's modulus of elasticity (N/m$^2$); e is the radius of the loaded area; $v$ is the Poisson's ratio.

Equations (1) to (8), denoted and illustrated in Table 3, are explained as follows below.

Equation (1) highlights the $y_m$ of a simply supported circular plate of diameter 2r under pressure $p$. The $D$ and $v$ have a great influence on the deformation of the plate. Therefore, the higher the $D$ of a plate, the less its deformation.

Equation (2) highlights the $y_m$ of a circular plate clamped at all edges with a diameter of 2r under pressure p. The $D$ and $v$ have a great influence on the deformation of the plate. Therefore, the higher the $D$ of a plate, the less its deformation.

Equation (3) highlights the $y_m$ of a simply supported circular plate of diameter 2r under force P over an area of radius e. The $D$ and the $v$ have a great influence on the plate. Therefore, the higher the $D$ of a plate, the less its deformation.

Equation (4) highlights the $y_m$ of a circular plate clamped at all edges with a diameter of 2r under force P over an area of radius e. The $D$ and the $v$ have a great influence on the plate. Therefore, the higher the $D$ of a plate, the less its deformation.

Equation (5) highlights the $y_m$ of a simply supported rectangular plate of dimensions a and b under pressure p. The $D$ and $v$ have a great influence on the deformation of the plate. Therefore, the higher the $D$ of a plate, the less its deformation.

Equation (6) highlights the $y_m$ of a rectangular plate of dimensions *a* and *b* clamped at all edges under pressure *p*. The *D* and *v* have a great influence on the deformation of the plate. Therefore, the higher the *D* of a plate, the less its deformation.

Equation (7) highlights the $y_m$ of a simply supported rectangular plate of dimensions a and b under force P over an area of radius e. The constant ($k_1$) is dependent on the aspect ratio (a/b) of the plate. Therefore, the greater the aspect ratio, the greater the deformation. Also, the *D* has a great influence on the deformation of the plate.

Equation (8) highlights the $y_m$ of a rectangular plate of dimensions a and b clamped at all edges under force P over an area of radius e. The constant ($k_1$) is dependent on the aspect ratio ($a/b$) of the plate. Therefore, the greater the aspect ratio, the greater the deformation. Also, the *D* has a great influence on the deformation of the plate.

*D* is the flexural rigidity, which is determined by solving Equation:

$$D = \frac{Et^3}{12\left(1-v^2\right)}. \tag{9}$$

Plates are susceptible to various types of failures under different loading conditions. Some of the common types of failures susceptible to plates include fatigue failure. Fatigue failure can occur in plate structures due to repeated cyclic loading, leading to the initiation and propagation of cracks in the material. This type of failure is a concern for structures subjected to varying magnitudes of loads, such as wind turbine towers or bridges. The study [17] examined the various factors affecting the fatigue strength of thin plates in large structures. Moreover, when the elastic limit of the plate material has been exceeded, this exceedance of the elastic limit can lead to ductile failure of the plate, also commonly known as yielding failure. Yielding failure results in the permanent deformation of the plate and occurs as a condition in which the compressive stress surpasses the material's yield strength.[12] The study [18] covered the prediction of yield failure points in notched aluminium plates. To study the ductile failure of the notched aluminium specimens, a brittle material with a virtual ultimate strength was used to compare with the real ductile material. Lastly, plate buckling is a phenomenon that occurs as a condition in which a thin plate moves out of the plane under a compressive load, causing it to bend in two directions [19].

### *1.2. Plate Buckling*

Structural members in compression are susceptible to failure by buckling if the applied compressive load exceeds the critical load (buckling load). Buckling failure is not dependent on stress or strength but rather on structural stiffness. Plates are buckled in orthogonal directions (see Figure 3) [19–21].

The major parameters influencing the buckling effect of plates include the aspect ratio ($a/b$), plate slenderness ($b/t$), boundary conditions, the initial imperfections of the plane, and, lastly, the type of plane loads.

The ratio of its longer side to its shorter side has a significant impact on its buckling behavior (Figure 4). For large aspect ratios, the plate starts behaving like a column of finite width. As the aspect ratio decreases, there is a limit below which failure does not take place by elastic buckling. The ratio affects the buckling load, with the buckling load decreasing continuously as the aspect ratio increases. However, the rate decreases with an increasing ratio. Additionally, for aspect ratios less than 0.5, the plates fail by crushing and not by buckling. Beyond a certain aspect ratio, the plate behavior shifts from plate to column [21–24].

[12] Investigations Into Steel Structure Failures Part I: Failure Mechanisms — Built Environment, Engineering Hawkins Forensic Investigation. (2022). Hawkins Forensic Investigation. Available from: https://www.hawkins.biz/insight/investigations-into-steel-structure-failures-part-i-failure-mechanisms/ (accessed: 03.04.2025).

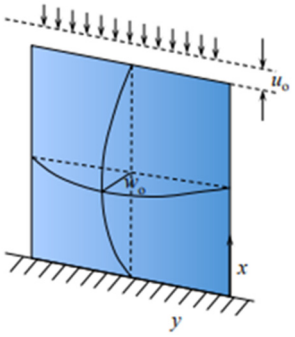


**Figure 3.** Two-degree-of-freedom model of the buckled plate
S o u r c e: compiled by T.Yu [22].

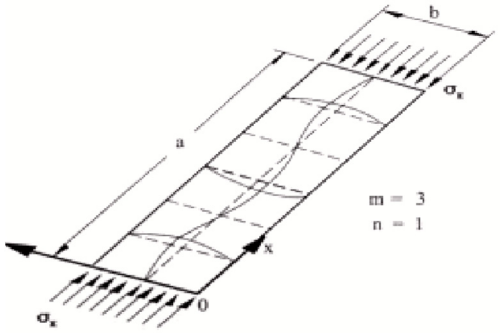


**Figure 4.** A plate with a high aspect ratio
S o u r c e: compiled by K.J. Rawson and E.C. Tupper [25].

In the design of plate structures, determining the thickness of the plate to be used to guard against buckling is crucial. For plate buckling, the Euler buckling limit is not final. Therefore, the Euler buckling stress is greater than the yielding stress. That is why, in plate design, an increase in the strength or grade of material must result in a decrease in the length of the plate. Higher-tensile-strength materials have an increasing risk of buckling [21; 22; 25; 27]. Equation (10) shows the critical buckling load of a supported rectangular plate:

$$N_{x_{cr}} = \frac{k_c \pi^2 D}{b^2}\ , \tag{10}$$

where $N_{x_{cr}}$ is the critical buckling load, $k_c$ is the buckling coefficient (see Figure 4 and Table 4), $b$ is the loaded length, and $D$ is flexural rigidity (see Equation (9)). The type of boundary support is an important factor that influences a plate's deformation and buckling loads, along with other factors such as modulus ratio, etc. The buckling load attains its minimum value under simply supported boundary conditions and its maximum value under clamped boundary conditions. This is because the rigidity of the clamped edges provides greater restraint against lateral deformation compared to the simply supported edges, thereby increasing the buckling load capacity.

*Table 4*

**Buckling coefficients of plates**

| Case | Description of support at the unloaded edges | | k |
|---|---|---|---|
| 1 | Both edges are simply supported | 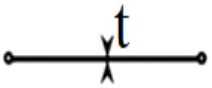 | 4.000 |
| 2 | One edge is simply supported, the other fixed | 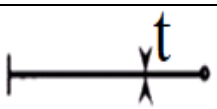 | 5.42 |
| 3 | Both edges are fixed | 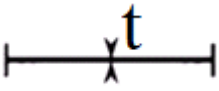 | 6.97 |
| 4 | One edge is simply supported, the other free | 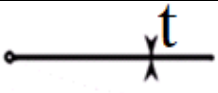 | 0.425 |
| 5 | One edge is fixed, the other free | 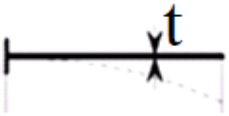 | 1.277 |

S o u r c e: compiled by U. Obinna [19].

The plate's boundary conditions and aspect ratio determine the plate's bending mode and the distance between inflection points. The closer the inflection points are, the greater the resulting axial load capacity (buckling load) of the plate. Therefore, it is essential to properly define the boundary conditions not only in the out-of-plane direction but also in the in-plane direction to accurately predict the buckling behavior of plates [19; 27]. Figure 5 shows how the aspect ratio affects the number of half-waves on the unloaded and longer axis (m). Furthermore, the aspect ratio determines how many half-waves or modes the plate will have during failure (see Figures 6–8). Figure 7 shows a plate with an aspect ratio of 3, producing 3 half-waves along the longer axis. Figure 8, on the other hand, shows a plate with 2 and a half waves along the longer axis.

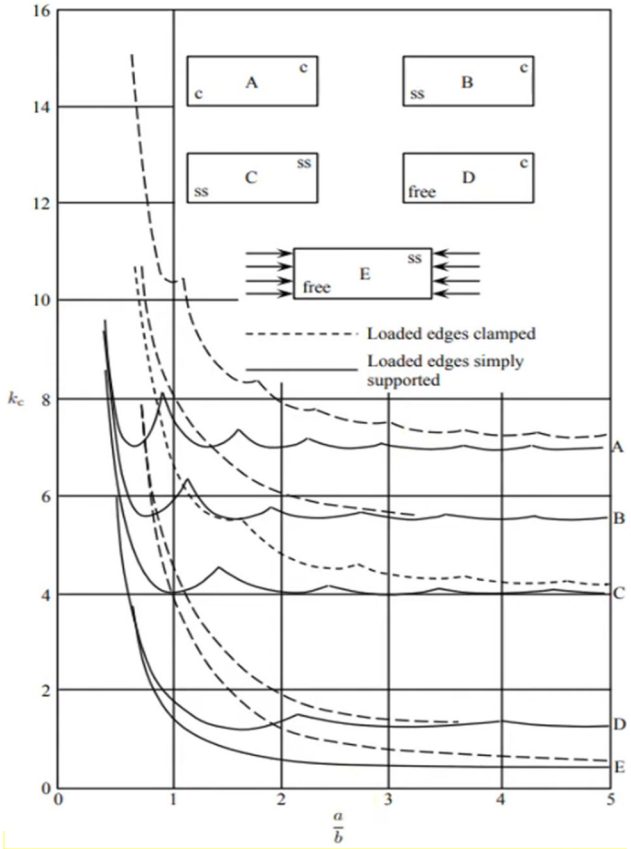


**Figure 5.** Buckling coefficient for different boundary conditions:
SS — denotes simply supported; C — denotes clamped
S o u r c e: compiled by O.M.E. Suleiman et al. [31].

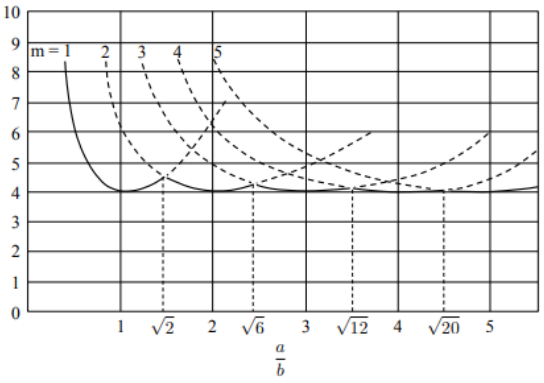


**Figure 6.** Buckling load as a function of aspect ratio for a simply supported plate
S o u r c e: compiled by T.Yu. [21]

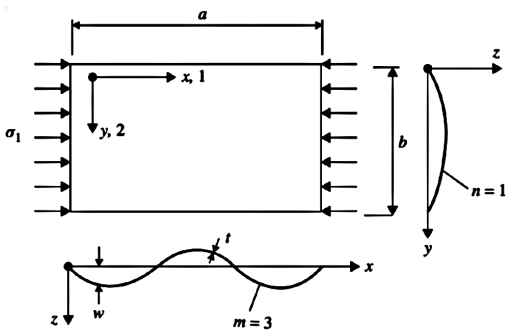


**Figure 7.** Simply supported plate buckling mode (3, 1)
S o u r c e: compiled by O.M.E. Suleiman et al. [31].

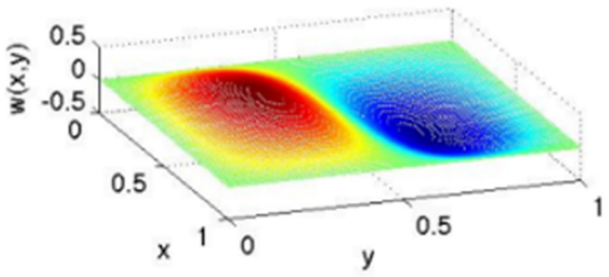


**Figure 8.** Buckling modes of a simply-supported thin plate — Mode (2, 1)
S o u r c e: compiled by T.Yu. [21].

### *1.3. Effect of Load Types and Combinations*

The type and combination of loads, as well as the boundary conditions, greatly affect the deformation of plates. Restricting in-plane deformation reduces the buckling load by a factor of 3/4, but it does not change the buckling mode. The buckling coefficient is a function of the loading distribution, plate geometry, and boundary conditions. The buckling interaction curve shows the effect of applied loads and boundary conditions for different modes of buckling on plates[13] [19; 28–30]. Figures 9–12 display 4 types of load combinations applied to plates[14].

If multiple action components are present, multiple modes can occur, which may interact with one another. Therefore, in Figure 10, the existence of minimal transverse compression does not alter the mode of buckling. Nonetheless, as illustrated in Figure 12, significant transverse compression will lead to the panel warping into a single half-wave. (In certain situations, this push into a higher mode could enhance strength; for instance, in case of Figure 12, preformation/ transverse compression might boost strength in longitudinal compression.) Shear buckling, illustrated in Figure 11, fundamentally involves an interplay between the destabilising compression on one diagonal and the stabilising tension on the opposite diagonal.

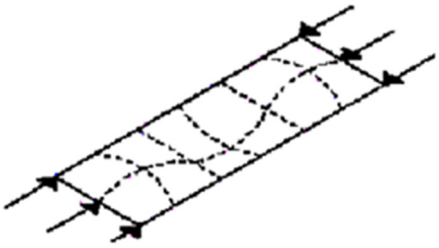

**Figure 9.** Uniaxial compression
S o u r c e: compiled by ESDEP WG 8 Plates and Shells.

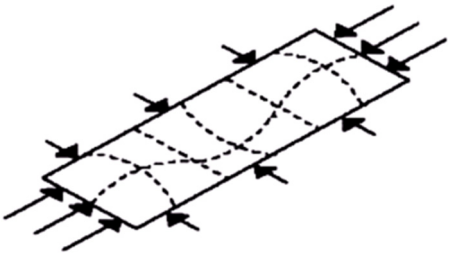

**Figure 10.** Biaxial compression, longitudinal compression predominating
S o u r c e: compiled by ESDEP WG 8 Plates and Shells.

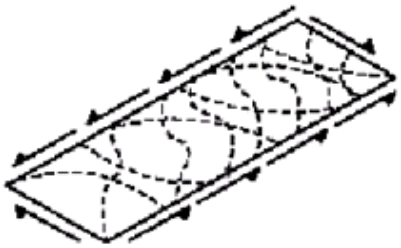

**Figure 11.** Shear
S o u r c e: compiled by ESDEP WG 8 Plates and Shells.

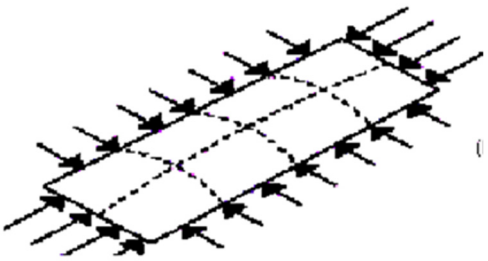

**Figure 12.** Biaxial compression, transverse compression predominating
S o u r c e: compiled by ESDEP WG 8 Plates and Shells.

### *1.4. Environmental Conditions*

Environmental conditions can affect thin plates in various ways, such as through changes in temperature, humidity, and exposure to different types of loads. For example, in the previously stated context of plate structures, the buckling strength is influenced by the loading distribution, plate geometry, and boundary conditions. Additionally, the material properties of the plate, including any dependence on environmental conditions, can impact its behavior under different loads and stresses. Therefore, it is

[13] Wierzbicki T. Buckling of a simply supported plate. Structural Mechanics, Massachusetts Institute of Technology, 170-181. file:///C:/Users/user/Downloads/Full.pdf

[14] ESDEP WG 8 Plates and Shells. Lecture 8.1: Introduction to Plate, Behaviour and Design. Available from: https://fgg-web.fgg.uni-lj.si/~/pmoze/esdep/master/wg08/l0100.htm (accessed: 03.04.2025).

essential to consider the specific environmental conditions and loading scenarios when analysing the behavior of thin plates to ensure their structural integrity and performance [31; 32].

The average annual temperature in most tropical savanna regions is 26.9°C, with regional variations based on factors such as elevation and proximity to water bodies. The highest average monthly temperatures are between 30 and 32 °C, typically occurring in April, while the lowest average monthly temperatures are between 24 and 25 °C, typically occurring in December and January. Over the past 30 years, tropical savanna regions have experienced a slight increase in temperature. For example, in 2021, southern Nigeria recorded a mean average temperature of 30 to 32°C, while the northern recorded its highest temperature in 40 years. This increase in temperature is consistent with other tropical savanna regions, i.e. Ghana, Southeast Asia, Northern Australia, Brazil, etc. and global climate change trends [33; 34].

The temperature resistance of structural aluminium alloys varies depending on the specific alloy and composition. However, most aluminium alloys begin to lose strength at temperatures above 150 °C (300 °F) [35; 36]. The primary strength reduction in some alloys, such as 5083-H116 and 6082, occurs between 200 and 400 °C, leading to significant decreases in yield strength [37; 38]. Although it was revealed that aluminium alloys perform better in both strength and ductility at low temperatures. The duration of exposure plays a crucial role for cold-worked or heat-treated alloys [37; 38]. Figure 13 highlights the change in typical tensile strengths of some aluminium alloys at various temperatures.

To find out how resistant a certain structural aluminium alloy is to high temperatures, one needs to look at the mechanical and physical properties of the aluminium alloy at those temperatures, which depend on its chemical makeup and temperature [40–42]. The thermal expansivity of materials is also a key factor that influences the behavior of plates.

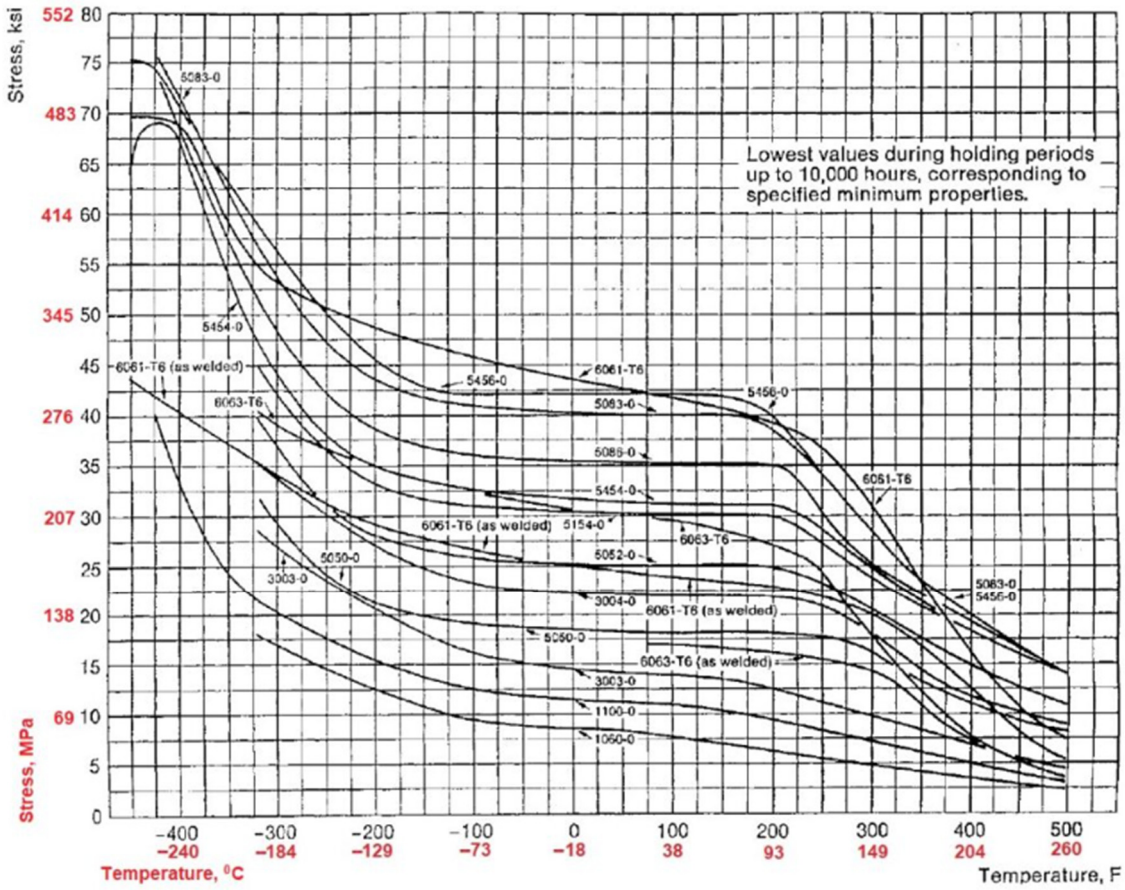


**Figure 13.** The strength of aluminium against temperature

S o u r c e: compiled by J.R. Kissell, R.L. Ferry [43].

### *1.5. Thermal Expansivity*

The thermal expansivity of materials is a key factor that influences the structural behaviour of plates [44; 45]. Equation (13) shows the change in length caused by a change in temperature in materials.

$$\Delta L = \alpha L_0 \Delta T, \tag{13}$$

where $\Delta L$ is the change in length; $\alpha$ is the linear thermal expansion coefficient; $L_0$ is the original length; $\Delta T$ is the change in temperature

The thermal expansion coefficient of aluminium is relatively large compared to other metals. Linear thermal expansion coefficients for aluminium and aluminium alloys are shown in Table 5. [15]

*Table 5*

**Coefficient of thermal expansion $10^{-6}\,(°\text{C})$ of aluminium alloys**

| Metal or alloy | Temp | Coefficient of thermal expansion $10^{-6}\,(°\text{C})$ |
|---|---|---|
| Aluminium (99.996%) | 20–100°C | 23.6 |
| 3003 | 20–100°C | 23.2 |
| 5083 | 20–100°C | 23.4 |

S o u r c e: compiled by Engineering ToolBox.

Moreover, Table 5 highlights the variety of coefficient of thermal expansion (CTE) of aluminium and its alloys. The secant CTE of aluminium and its alloys also varies. The secant CTE is a measure that accounts for the change in length or volume of a material over a specific temperature range. Unlike the linear CTE, which provides a constant value for the entire temperature range, the secant CTE calculates the average thermal expansion over a specified temperature interval. A commonly used average value for the linear CTE of aluminium is approximately $23\times10^{-6}$ per degree Celsius (°C).

### *1.6. Importance of Aluminium*

The transformation of discarded aluminium cans into valuable construction components aligns with the global shift towards resource efficiency and circular economy principles. The feasibility of this transformation poses several questions:

i. Can aluminium cans be effectively turned into structurally sound aluminium plates?
ii. Will these plates meet the structural requirements in terms of strength, durability, and safety?

Several studies have examined the mechanical and thermal behavior of steel and aluminium alloys; most were conducted under normal or temperate climatic conditions, with comparably few examinations of the materials' thermomechanical performance under tropical savanna climatic conditions. Additionally, previous research tended to examine deformation or buckling separately from one another, as opposed to concurrent analyses of the two in a representative range of thermal fluctuations. This study differs from existing literature by examining the coupled deformation–buckling behavior of recycled aluminium and steel plates under simulated tropical temperature variations (0°C–44°C) using finite element analysis (FEA). Thus, this paper aims to unravel the potential of aluminium plates by scrutinising their mechanical, thermal, and structural properties, to understand how the change in temperature affects the deformation and buckling of plates under loading. Hence, the objective of this is as follows:

[15] Engineering ToolBox. (2011). Thermal Expansion of Metals. Engineeringtoolbox.com. https://www.engineeringtoolbox.com/thermal-expansion-metals-d_859.html

i. Ensure the analytical theories agree with the finite element analysis (FEA) results
ii. To determine the deformation of the plate models under various loads and temperature conditions.
iii. To define how the change in temperature affects the critical buckling of the plates.

## 2. Materials and Models

Three analysis systems were used in this study, all done on the Ansys workbench software, i.e. Steady-state Thermal, Static Structural, and Eigenvalue Buckling. The geometrical model was created by the design modeller (see Figure 14). A circular surface was imprinted at the centre of the plate using the Boolean tool, highlighting where the load would be placed for analysis 1 (see Figure 15). A shell element model type was used with a 30 mm thickness (see Figure 15–16). Both faces were meshed using a meshing element size of 200 mm.

### *2.1. Material Properties*

The physical and mechanical properties used for both plates (aluminium alloy and steel alloy) are summarised in Table 6.

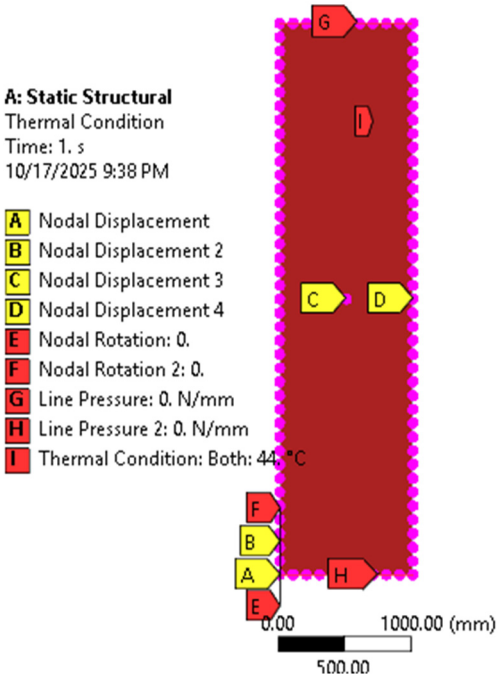


**Figure 14.** Analysis systems used
S o u r c e: compiled by P.C. Chiadighikaobi, O.C. Onuoha, A.E. Fagbuyi.

*Table 6*

**Physical and mechanical properties of aluminium and steel**

| Properties | Symbol | Aluminium alloy | Steel alloy |
|---|---|---|---|
| Density, kg/m$^3$ | $Q$ | 2,770 | 7,850 |
| Elastic modulus, MPa | $E$ | 71,000 | 200,000 |
| Poisson's ratio | $v$ | 0.33 | 0.3 |
| Yield strength, MPa | $Ru$ | 280 | 250 |
| Secant coefficient of thermal expansion | $10^{-6}$ (°C)$^{-1}$ | 23 | 12 |

S o u r c e: compiled by P.C. Chiadighikaobi, O.C. Onuoha, A.E. Fagbuyi.

### *2.2. Supports and Loading*

Both plates were simply supported. All the nodes at the edges were restrained along the z-axis, the nodes on the longer sides were free to rotate about z- and y-axis, but fixed along the x-axis, while the nodes on the shorter sides were free to rotate about z- and x-axis, but fixed along the y-axis. Lastly, the node at the centre was fixed along both the x- and y-axis. In addition, the loads placed were dependent on the analysis.

*Table 7*

**The 5 levels of uniform loading**

| S/N | Loads, MPa |
|---|---|
| 1 | 0 |
| 2 | 25 |
| 3 | 50 |
| 4 | 75 |
| 5 | 100 |

S o u r c e: compiled by P.C. Chiadighikaobi, O.C. Onuoha, A.E. Fagbuyi.

**A n a l y s i s 1: Temperature-Influenced Deformation of Plates Under Concentrated Load.** In this analysis, five (5) levels of uniform loading (Table 7) were applied to the circular area (diameter = 9 mm) at the centre of the plate (see Figure 15).

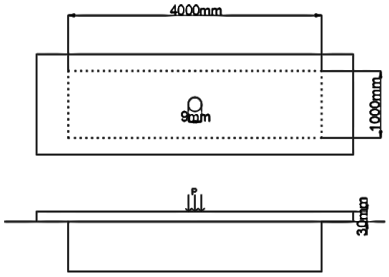


**Figure 15.** Analysis 1:
plate and loading area dimensions
S o u r c e: compiled by P.C. Chiadighikaobi, O.C. Onuoha, A.E. Fagbuyi.

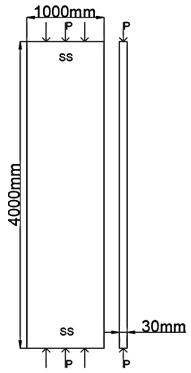


**Figure 16.** Analysis 2:
plate and loading area dimensions
S o u r c e: compiled by P.C. Chiadighikaobi, O.C. Onuoha, A.E. Fagbuyi.

*Table 8*

**The 7 different temperatures**

| S/N | 1 | 2 | 3 | 4 | 5 |
|---|---|---|---|---|---|
| **Temperature, °C** | 0 | 11 | 22 | 33 | 44 |

S o u r c e: compiled by P.C. Chiadighikaobi, O.C. Onuoha, A.E. Fagbuyi.

**Analysis 2: Total Buckling Deformation of the Plate.** In this case, the plate was subjected to a uniaxial compressive force along the y-axis (see Figure 16). The loads were applied as line pressure, and the load applied was 10000 N/m. In addition, with the aspect ratio being four, the first mode is expected to have four half-waves.

### *2.3. Temperature Conditions*

The plates were subjected to 6 (six) different temperatures during loading in both analyses.

The reference temperature used was 22°C (Table 8).

## 3. Results

The FEA results for Analyses 1 and 2 are stated in this section below.

**Analysis 1 result: Temperature Influenced Deformation**. The derived FEA deformation results validate the formulae stated in the previous section, i.e. Equations (7) and (13). Using Equation (13), the expected total maximum deformation (TMD) for the unloaded 33 °C plate was 0.506 mm (2 × 0.253 mm) for aluminium and 0.264 mm (2 × 0.132 mm) for Steel. Tables 9 and 10 show that the TMD was 0.5216 mm and 0.27214 mm, respectively. In addition, the Equation (7) derived TMD for 25 °C plates under 100 MPa load were 0.60798 mm for aluminium and 0.21583 mm for steel. While Tables 8 and 9 show the TMD was 0.57823 mm and 0.2095 mm. These results are quite precise with less than a 5-percentile difference. Hence, proving the accuracy of the FEA results.

*Table 9*

**Aluminium plate: total maximum deformation**

| | 0°C | 11°C | 22°C | 33°C | 44°C |
|---|---|---|---|---|---|
| **0 MPa** | 0.97516mm | 0.50629mm | 0mm | 0.5216mm | 1.0432mm |
| **25 MPa** | 0.97516mm | 0.50629mm | 0.14456mm | 0.5216mm | 1.0432mm |
| **50 MPa** | 0.97516mm | 0.50629mm | 0.28900mm | 0.5216mm | 1.0432mm |
| **75 MPa** | 0.97516mm | 0.50629mm | 0.43368mm | 0.5216mm | 1.0432mm |
| **100 MPa** | 0.97516mm | 0.57823mm | 0.57823mm | 0.57823mm | 1.0432mm |

S o u r c e: compiled by P.C. Chiadighikaobi, O.C. Onuoha, A.E. Fagbuyi.

*Table 10*

**Steel plate: total maximum deformation**

| | 0°C | 11°C | 22°C | 33°C | 44°C |
|---|---|---|---|---|---|
| **0 MPa** | 0.49892mm | 0.26193mm | 0mm | 0.27214mm | 0.54428mm |
| **25 MPa** | 0.49892mm | 0.26193mm | 0.05240mm | 0.27214mm | 0.54428mm |
| **50 MPa** | 0.49892mm | 0.26193mm | 0.10475mm | 0.27214mm | 0.54428mm |
| **75 MPa** | 0.49892mm | 0.26193mm | 0.15712mm | 0.27214mm | 0.54428mm |
| **100 MPa** | 0.49892mm | 0.26193mm | 0.2095mm | 0.27214mm | 0.54428mm |

S o u r c e: compiled by P.C. Chiadighikaobi, O.C. Onuoha, A.E. Fagbuyi.

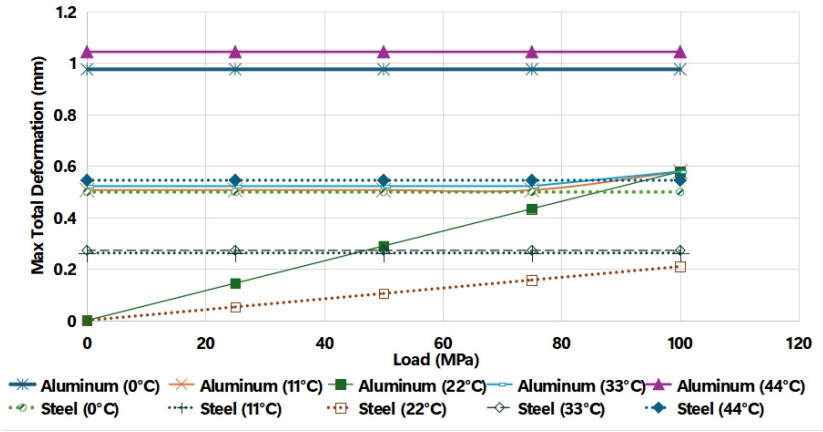


**Figure 17.** Total maximum deformation of aluminium and steel plates

S o u r c e: compiled by P.C. Chiadighikaobi, O.C. Onuoha, A.E. Fagbuyi.

Figure 17 shows that the TMD of plates at various temperature, except the ones at reference temperature (22 °C), are greatly dependent on the temperature of the plate and not the load acting on it. The aluminium and steel plate TMD remained constant at 0 °C, 11 °C, 33 °C, and 44 °C, particularly under the condition where the applied load was less than 100 MPa. Moreover, as seen in Figure 18, the unloaded 0 °C aluminium plate (a) and steel plate (c) TMD point is at the bottom corner of the plate, and after the 100 MPa load was applied on aluminium plate (*b*) and steel plate (*d*), the TMD point was retained. In addition, the mid node total deformation of 0 °C plates under 100 MPa loading was 0.42115 mm for aluminium and 0.20825 mm for steel, both lower than the mid node deformations at the reference temperature (22 °C), which is 0.57823 mm and 0.2095 mm, respectively (see Figure 19). Thus, proving aluminium slight gain in strength at lower temperatures. Validating the study Guo et al. [46], which stated that low temperatures improved both strength and ductility of aluminium, while higher temperatures reduced the strength due to softening. In addition, the plates (aluminium and steel) at lower temperatures (0 °C and 11 °C) deformed by contracting, while the plates at higher temperatures (33 °C and 44 °C) deformed my expanding. Thus, proving why the loaded plate mid-node total deformation was more at higher temperatures than at lower temperatures. In Figure 20, *b* and *d* total mid node deformation was 0.57823 mm and 0.22573 mm, respectively, which is higher than the other temperature cases.

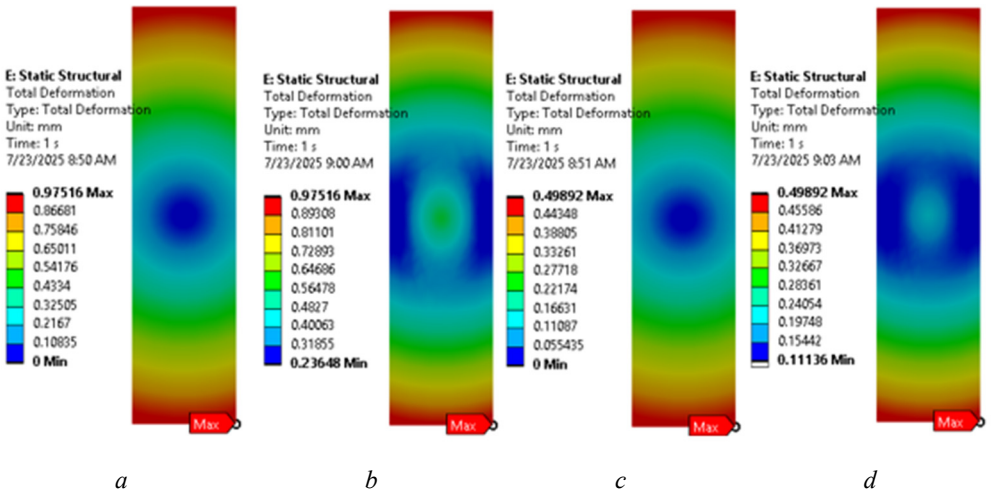


*a* *b* *c* *d*

**Figure 18.** Total maximum deformation for unloaded and loaded 0 °C plates:
*a* — Aluminium; *b* — Aluminium; *c* — Steel; *d* —Steel

S o u r c e: compiled by P.C. Chiadighikaobi, O.C. Onuoha, A.E. Fagbuyi.

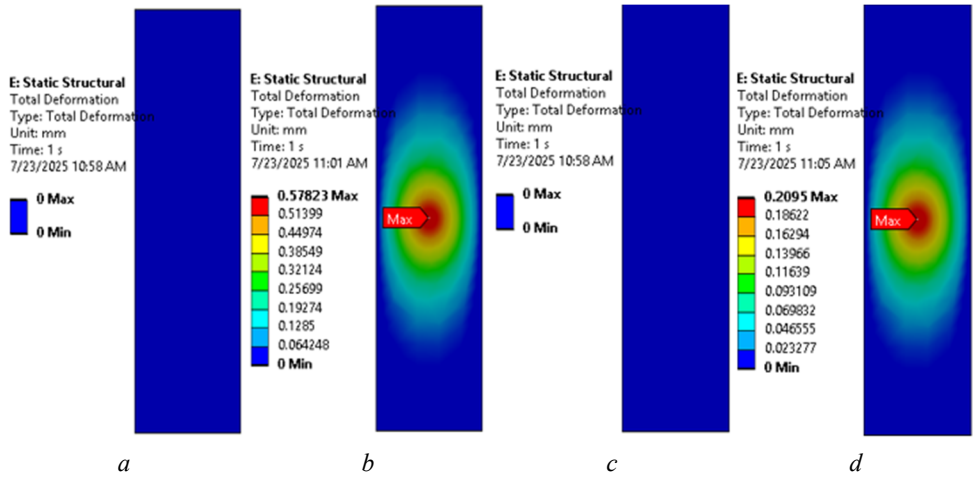


**Figure 19.** Total maximum deformation for unloaded and loaded 22 °C plates:
*a* — Aluminium; *b* — Aluminium; *c* — Steel; *d* — Steel
S o u r c e: compiled by P.C. Chiadighikaobi, O.C. Onuoha, A.E. Fagbuyi.

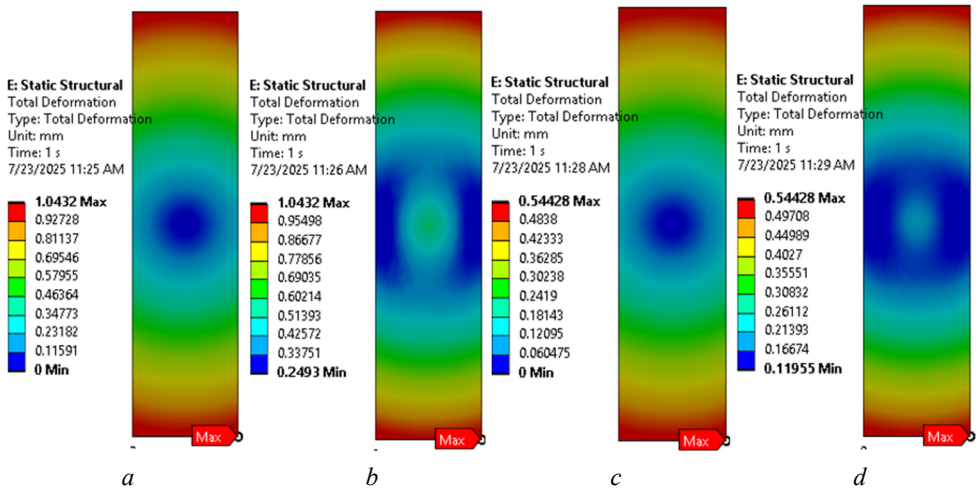


**Figure 20.** Total maximum deformation for unloaded and loaded 44 °C plates:
*a* — Aluminium; *b* — Aluminium; *c* — Steel; *d* — Steel
S o u r c e: compiled by P.C. Chiadighikaobi, O.C. Onuoha, A.E. Fagbuyi.

**Analysis 2 Result: Temperature Influenced Buckling.** The FEA buckling results accuracy was validated by equation (10). Equation (10) derived buckling load for plates at reference temperature was 7,070,232 N/m for aluminium and 19,502,505 N/m for steel, while the FEA load was 7,330,000 N/m and 20,237,000 N/m (see Table 10). The results are quite precise with less than a four-percentile difference. Thus, proving accuracy of the FEA method used.

*Table 10*

**Critical buckling load results**

| | Aluminium | | Steel | |
|---|---|---|---|---|
| | **Mode 1** | **Mode 2** | **Mode 1** | **Mode 2** |
| **Uniaxial Compression Load, 10,000 N/m** | | | | |
| **0 °C** | –761.76 | 733.5 | –1576 | 2024.1 |
| **11 °C** | 733.47 | 781.16 | 2024.1 | 2155.6 |
| **22 °C** | 733.33 | 781.29 | 2023.7 | 2156.1 |
| **33 °C** | 732.89 | 781.43 | 2020.3 | 2156.7 |
| **44 °C** | 699.88 | 739.80 | 1435.6 | 1856.3 |

S o u r c e: compiled by P.C. Chiadighikaobi, O.C. Onuoha, A.E. Fagbuyi.

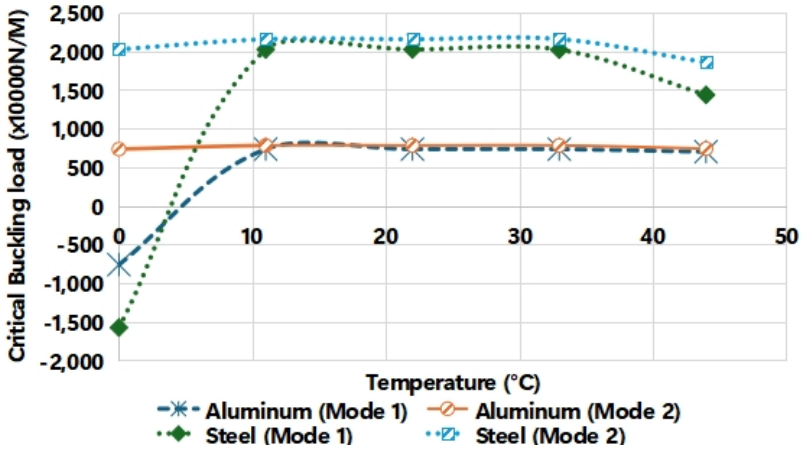


**Figure 21.** Critical buckling of uniaxially compressed plates
S o u r c e: compiled by P.C. Chiadighikaobi, O.C. Onuoha, A.E. Fagbuyi.

Figure 21 shows that both plates mode 1 critical buckling load is quite temperature sensitive, with the higher buckling loads observed near the reference temperature. At mode 1, the steel critical bulking load significantly dropped by 40.7% due to the temperature change from 33 °C to 44 °C (see Figure 24), while aluminium dropped only by 4.71%. A similar phenomenon was observed in mode 2, where the critical buckling load for the steel plate dropped by 16.18% when the temperature changed from 33 °C to 44 °C (see Figure 24), while aluminium dropped 5.63%. Validating that, despite the buckling mode, the steel critical buckling load is much more sensitive to temperature than aluminium. In addition, it was observed that despite the mode, the plates at 0 °C and 44 °C had no more than 4 half-wavelengths. While for mode 2 plates closer to the reference temperature (22°C), an additional wavelength was formed (see Figure 23). Hence proving that the environmental temperature plays a crucial role in plate buckling modes (see Figure 24).

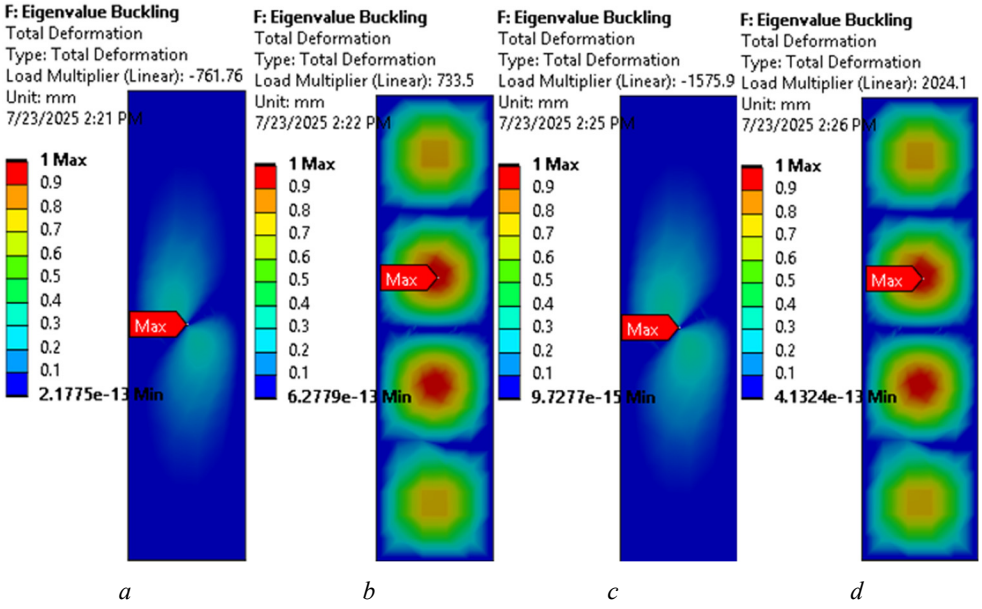


**Figure 22.** Buckling deformation of plates at 0 °C:
*a* — Aluminium (mode 1); *b* — Aluminium (mode 2); *c* — Steel (mode 1); *d* — Steel (mode 2)
S o u r c e: compiled by P.C. Chiadighikaobi, O.C. Onuoha, A.E. Fagbuyi.

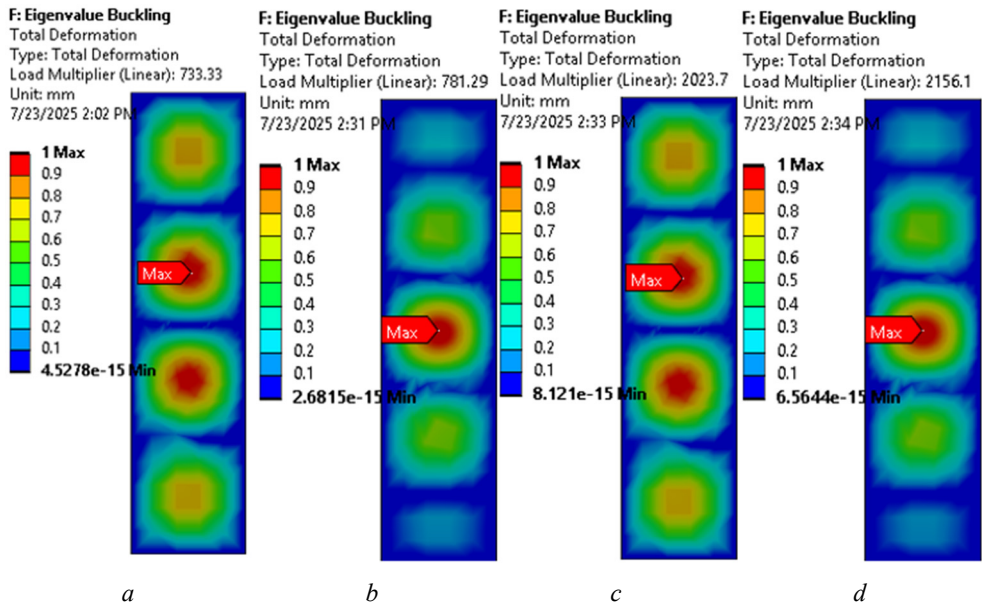


*a* *b* *c* *d*

**Figure 23.** Buckling deformation of plates at 22 °C:
*a* — Aluminium (mode 1); *b* — Aluminium (mode 2); *c* — Steel (mode 1); *d* — Steel (mode 2)
S o u r c e: compiled by P.C. Chiadighikaobi, O.C. Onuoha, A.E. Fagbuyi.

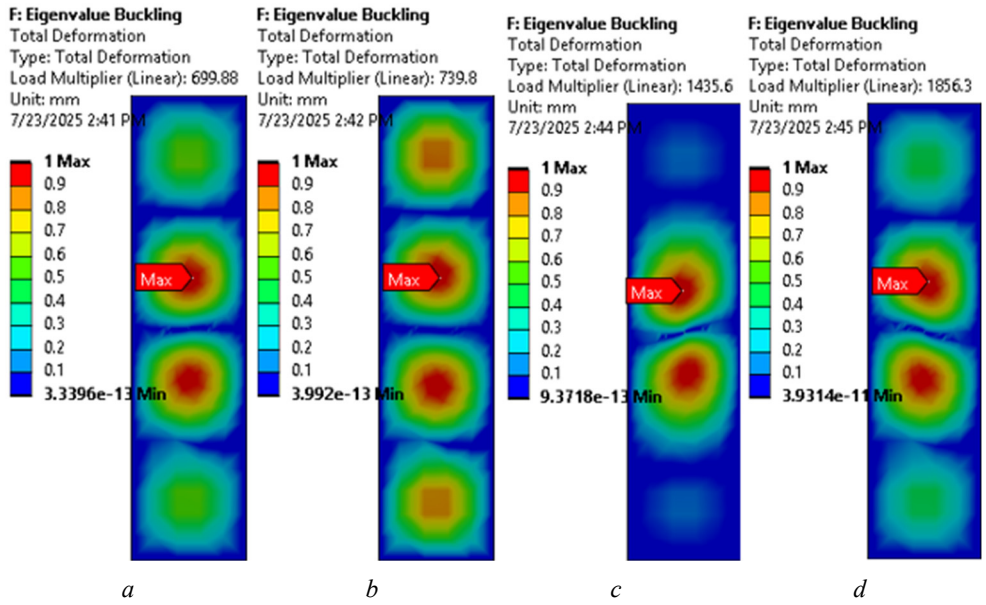


*a* *b* *c* *d*

**Figure 24.** Buckling deformation of plates at 44 °C:
*a* — Aluminium (mode 1); *b* — Aluminium (mode 2); *c* — Steel (mode 1); *d* — Steel (mode 2)
S o u r c e: compiled by P.C. Chiadighikaobi, O.C. Onuoha, A.E. Fagbuyi.

## 4. Conclusion

In conclusion, this study illuminates the potential for aluminium as a suitable construction material. The finite element analysis (FEA) results agreed with their analytical formulations with less than 5 percentile difference, thus proving the efficiency of FEA. The conclusive findings of this study are as follows.

1. The results showed that aluminium plates experienced slightly greater overall maximum deformation than steel under every temperature and loading condition. However, aluminium was discovered to be more thermally stable. At low temperatures (0° C and 11 °C), aluminium experienced lesser deformation, with mid-node deformation going down to 0.42115 mm under 100 MPa, whereas 0.57823 mm at the reference

temperature (22°C). Steel also performed well at low temperatures, but with minimal change in mid-node deformation.

2. Under buckling analysis, aluminium experienced stable performance with a reduction of just 4.71% in critical buckling load between 33 °C and 44 °C. Steel's critical buckling load in Mode 1, on the other hand, dropped precipitously by 40.7% over the same temperature range, illustrating its vulnerability to temperature change. Mode 2's results also indicated a lower but noticeable drop in steel performance, whereas aluminium again remained relatively stable.

These findings show that while steel offers higher stiffness and lower deformation at moderate conditions, recycled aluminium offers a better performance under large temperature fluctuations, thus highlighting its potential as a viable material for enhancing thermal and structural efficiency in a hot climate.

## References

1. Eze F.O., Nnamani E. Effective supply chain network: A sustainable approach to waste management in South-Eastern Nigeria. *International Digital Organization for Scientific Research Journal of Applied Sciences*. 2019;4(1):74–85. Available from: https://www.idosr.org/wp-content/uploads/2019/04/IDOSR-JAS-41-74-85-2019.pdf (accessed: 03.04.2025).

2. Risonarta V.Y., Anggono J., Suhendra Y.M., Nugrowibowo S., Jani Y. Strategy to improve recycling yield of aluminium cans. *E3S Web of Conferences*. 2019;130:01033. https://doi.org/10.1051/e3sconf/201913001033

3. Wallace G. Production of secondary aluminium. In: *Elsevier eBooks*. 2011. p. 70–82. https://doi.org/10.1533/9780857090256.1.70

4. Falde N., Falde N. How is Aluminium Recycled? Step by Step | Greentumble. Greentumble. 2020. Available from: https://greentumble.com/how-is-Aluminium-recycled (accessed: 03.04.2025).

5. Nunes H., Emadinia O., Soares R., Vieira M.F., Reis A. Adding Value to Secondary Aluminium Casting Alloys: A review on Trends and Achievements. *Materials*. 2023;16(3):895. https://doi.org/10.3390/ma16030895 EDN: WAVSVT

6. Brough D., Jouhara H. The aluminium industry: A review on state-of-the-art technologies, environmental impacts and possibilities for waste heat recovery. *International Journal of Thermofluids*. 2020;1–2:100007. https://doi.org/10.1016/j.ijft.2019.100007 EDN: IRGUBX

7. Zuo Z., Liu Y., Kang J., Yu G., Liu F., Zhao H. Basic physical properties of Aluminium alloys and their electrolyte systems prepared by Molten Salt electrolysis using black Aluminium dross as raw material. *JOM*. 2022;74(5):2037–2046. https://doi.org/10.1007/s11837-021-05149-0

8. Mazzolani F.M. *Structural applications of aluminium in civil engineering. Structural Engineering International.* 2006;16(4):280–285. https://doi.org/10.2749/101686606778995128

9. Kissell J.R., Ziemian R.D. *The 2020 Aluminium Design Manual*. Trinity Consultants, Bucknell University. 2019; 77(4):2.

10. Mittelstedt C. Introduction to shell structures. In: *Springer eBooks*. 2023. p. 477–490. https://doi.org/10.1007/978-3-662-66805-4_14

11. Steele C.R., Balch C.D. *Introduction to the Theory of Plates.* Stanford University. Retrieved 2020-12-14. 2009.

12. Ali M.M., Al-Kodmany K. Structural systems for tall buildings. *Encyclopedia.* 2022;2(3):1260–1286. https://doi.org/10.3390/encyclopedia2030085

13. Arslan E., Kayaturk D., Durmus M.R., Bagca I., Imamoglu T., Sert S. The role of utilizing load in different cases while numerical modeling of multi-story buildings on alluvial stratum: a comparison study. *Arabian Journal for Science and Engineering*. 2024;49(10):13845–13860. https://doi.org/10.1007/s13369-024-08800-5

14. Van A.L. Reissner-Mindlin Plate Theory. In: *Elsevier eBooks*. 2017. p. 67–82. https://doi.org/10.1016/b978-1-78548-227-4.50004-6

15. Abrate S. Impact on composite plates in contact with water. *Dynamic Response and Failure of Composite Materials and Structures.* In: *Elsevier eBooks*. 2017. p. 183–216. https://doi.org/10.1016/b978-0-08-100887-4.00006-8

16. Wang C., Reddy J., Lee K. Chapter 1 — Introduction. Shear Deformable Beams and Plates Relationships with Classical Solutions 2000. p. 1–7. https://doi.org/10.1016/b978-008043784-2/50001-0

17. Johnson D. *Advanced structural mechanics: an introduction to continuum mechanics and structural mechanics*. Nottingham Trent University. Thomas Telford; 2010. ISBN 0 7277 2860 1

18. Remes H., Romanoff J., Lillemäe I., Frank D., Liinalampi S., Lehto P., & Varsta P. Factors affecting the fatigue strength of thin-plates in large structures. *International Journal of Fatigue*. 2026;101:397–407. https://doi.org/10.1016/j.ijfatigue.2016.11.019

19. Torabi A.R., Campagnolo A., Berto F. Large-Scale yielding failure prediction of notched ductile plates by means of the linear elastic notch fracture mechanics. *Strength of Materials.* 2017;49(2):224–233. https://doi.org/10.1007/s11223-017-9861-9 EDN: RREBNY

20. Obinna U. Buckling of Thin Plates — Structville. 2022. Available from: https://structville.com/2022/05/buckling-of-thin-plates.html (accessed: 03.04.2025).

21. Audoly B. Buckling and Post-buckling of Plates. *Encyclopedia of Continuum Mechanics*. 2020. p. 222–237. https://doi.org/10.1007/978-3-662-55771-6_134

22. Yu T. Buckling of Thin Plate. University of Massachusetts Lowell, Lowell, Massachusetts. 2017.

23. Quiel S.E., Moreyra E. Calculating the buckling strength of steel plates exposed to fire. *Thin-Walled Structures*. 2010;48(9):684–695. https://doi.org/10.1016/j.tws.2010.04.001 EDN: OEJYKD

24. Traub L.W. Examination and Prediction of the Lift Components of Low Aspect Ratio Rectangular Flat Plate Wings. *Aerospace*. 2023;10(7):597. https://doi.org/10.3390/aerospace10070597 EDN: ZSODWT

25. Rawson K.J., Tupper E.C. 7 — Structural design and analysis. *Basic Ship Theory (Fifth Edition)*. 2001. p. 237–285. https://doi.org/10.1016/B978-075065398-5/50010-8

26. Shrivastava A., Singh R. Effect of aspect ratio on buckling of composite plates. *Composites Science and Technology*. 1999;59(3):439–445. https://doi.org/10.1016/s0266-3538(98)00087-6

27. El-Sawy K.M., Nazmy A.S. Effect of aspect ratio on the elastic buckling of uniaxially loaded plates with eccentric holes. *Thin-Walled Structures*. 2001;39(12):983–998. https://doi.org/10.1016/s0263-8231(01)00040-4

28. Panda S.K., Ramachandra L. Buckling of rectangular plates with various boundary conditions loaded by non-uniform inplane loads. *International Journal of Mechanical Sciences*. 2010;52(6):819–828. https://doi.org/10.1016/j.ijmecsci.2010.01.009

29. Wang C., Liu Q. Buckling behaviour of rectangular and skew plates with elastically restrained edges under non-uniform mechanical edge loading. *PLoS ONE*. 2024;19(9):e0308245–e0308245. https://doi.org/10.1371/journal.pone.0308245 EDN: VXQKWY

30. Prabowo A.R., Ridwan R., Muttaqie T. On the Resistance to Buckling Loads of Idealized Hull Structures: FE Analysis on Designed-Stiffened Plates. *Designs*. 2022;6(3):46. https://doi.org/10.3390/designs6030046 EDN: PCPUXW

31. Suleiman O.M.E., Osman M.Y., & Hassan T. Effect of Boundary Conditions on Buckling Load for Laminated Composite Plates. *Global Journal of Engineering Sciences*. 2019;2(1). https://doi.org/10.33552/gjes.2019.02.000527

32. Shi P., Viet N., Yang J., Shou H., Li Q., Turan F. Free vibration and nonlinear transient analysis of blast-loaded FGM sandwich plates with stepped face sheets: Analytical and artificial neural network approaches. *Thin-Walled Structures*. 2024;206:112667–112667. https://doi.org/10.1016/j.tws.2024.112667 EDN: FZZWTS

33. Ren G., Pan R., Sun F., Dong Z., Lan T. Advanced Analysis of Structural Performance in Novel Steel-Plate Concrete Containment Structures. *Buildings*. 2024;14(9):2771–2771. https://doi.org/10.3390/buildings14092771 EDN: BCHYZI

34. Atuma I.M., Efe S.I., Ndakara O.E. Temperature trend in Niger Delta Region, Nigeria. *Journal of Management and Social Science Research*. 2023;4(1):29–39. https://doi.org/10.47524/jmssr.v4i1.30 EDN: JNEOPB

35. Stresman G.H. Beyond temperature and precipitation: Ecological risk factors that modify malaria transmission. *Acta Tropica*. 2010;116(3):167–172. https://doi.org/10.1016/j.actatropica.2010.08.005

36. Czerwinski F. Thermal stability of Aluminium alloys. *Materials*. 2020;13(15):3441. https://doi.org/10.3390/ma13153441 EDN: ZVPFGE

37. Rajaram G., Kumaran S., Rao T.S. High temperature tensile and wear behaviour of Aluminium silicon alloy. *Materials Science and Engineering A*. 2010;528(1):247–253. https://doi.org/10.1016/j.msea.2010.09.020

38. Summers P.T., Chen Y., Rippe C.M., Allen B., Mouritz A.P., Case S.W., Lattimer B.Y. Overview of Aluminium alloy mechanical properties during and after fires. *Fire Science Reviews*. 2015;4(1). https://doi.org/10.1186/s40038-015-0007-5

39. Lemmon A., Weritz J. *Fire Safety of Aluminium & Its Alloys*. The Aluminium Association. 2021. Available from: https://www.Aluminium.org/sites/default/files/2021-11/FireSafetyAluminiumAlloys_9.8.20.pdf (accessed: 03.04.2025).

40. Guo X., Tao L., Zhu S., Zong S. Experimental investigation of mechanical properties of Aluminium alloy at high and low temperatures. *Journal of Materials in Civil Engineering*. 2019;32(2). https://doi.org/10.1061/(asce)mt.1943-5533.0003002 EDN: HOHMZH

41. Su M., Young B. 10.37: Mechanical properties of high strength aluminium alloy at elevated temperatures. *Special Issue:Proceedings of Eurosteel 2017. Ce/Papers*. 2017;1(2–3):2831–2839. https://doi.org/10.1002/cepa.334

42. Sharma R., Sharma K., Saraswat B.K. A review of the mechanical and chemical properties of aluminium alloys AA6262 T6 and its composites for turning process in the CNC. *Materials Today: Proceedings*. 2023. https://doi.org/10.1016/j.matpr.2023.01.421 EDN: MHBYWF

43. Kissell J.R., Ferry R.L. *Aluminium Structures: A Guide to Their Specifications and Design*. John Wiley & Sons. 2002. ISBN 978-0-471-01965-7

44. Baytak T., Tosun M., Ipek C., Mollamahmutoglu C., Bulut O. Thermal Stress Analysis for Functionally Graded Plates with Modulus Gradation, Part II. *Experimental Mechanics*. 2024;64(8):1229–1247. https://doi.org/10.1007/s11340-024-01091-9 EDN: TECQLZ

45. Zhang H. *Building Materials in Civil Engineering*. Woodhead Publishing Series in Civil and Structural Engineering, 2011;423:7–28. ISBN 161344351X, 9781613443514

46. Guo X., Tao L., Zhu S., Zong S. Experimental investigation of mechanical properties of Aluminium alloy at high and low temperatures. *Journal of Materials in Civil Engineering*. 2020;32(2):06019016. https://doi.org/10.1061/(asce)mt.1943-5533.0003002 EDN: HOHMZH